Journal of Physics: Conference Series **556** (2014) 012007 doi:10.1088/1742-6596/556/1/012007

Spin observables in antihyperon-hyperon production with PANDA

K Schönning and E Thomé for the PANDA collaboration

Dept. of Physics and Astronomy, Uppsala University, Box 516, S-751 20 Uppsala, Sweden

E-mail: karin.schonning@physics.uu.se

Abstract. Spin observables provide a powerful tool in understanding the physics. Seven polarisation parameters of the Ω baryon can be extracted from the angular distributions of the hyperon decay and studied with the future PANDA experiment at FAIR. Simulation studies show that strange and single charmed hyperon channels have great prospects with PANDA.

1. Introduction

Hyperon production in $\overline{p}p \rightarrow \overline{Y}Y$ reactions gives important insights into strangeness and charm production. In this work, we consider single-, multi-strange and single-charmed hyperons. Their production from the light quarks in $\overline{p}p$ implies processes where they are replaced by heavier quarks. The relevant degrees of freedom of a given process are given by its energy scale, which for strangeness production is fixed by the mass of the strange quark, $m_s \approx 100$ MeV. This is close to the QCD cut-off, $\Lambda_{QCD} \approx 200$ MeV, where the strong coupling constant α_s grows so large that perturbative QCD breaks down. The production of strange hyperons can therefore probe QCD in the region below the perturbative regime, *i.e.* the confinement domain, about which very little is known so far. The scale of charm production is governed by $m_c \approx 1300$ MeV, more than ten times larger than m_s. The strong coupling constant in this region is $\alpha_s \approx 0.3$, just barely enough for a perturbative treatment to be valid. Comparing the production of strange and charmed hyperons could therefore give important insights into the differences in the production mechanism at these two energy scales. Theoretical models describing hyperon production in $\overline{p}p \rightarrow \overline{Y}Y$ reactions are often based on a constituent quark-gluon picture [1]. For strange hyperons, Kaon exchange models enter into play, where the production of single (multiple) strangeness hyperons are modeled by the single (multiple) exchange of a t-channel Kaon [2]. There have also been attempts to combine a quark-gluon approach with a Kaon exchange approach [3]. Spin variables are often very powerful in discriminating between different theoretical models. The hyperon spin variables can be related to the spin of individual quarks. The Λ hyperon can be modeled by a ud spin zero di-quark combined with an s-quark that carries the spin of the hyperon. A similar picture can be drawn for the Λ_c^+ hyperon, and by comparing spin observables of Λ and Λ_c^+, we can learn about the role of spin degrees of freedom in the creation of s- and c-quarks.

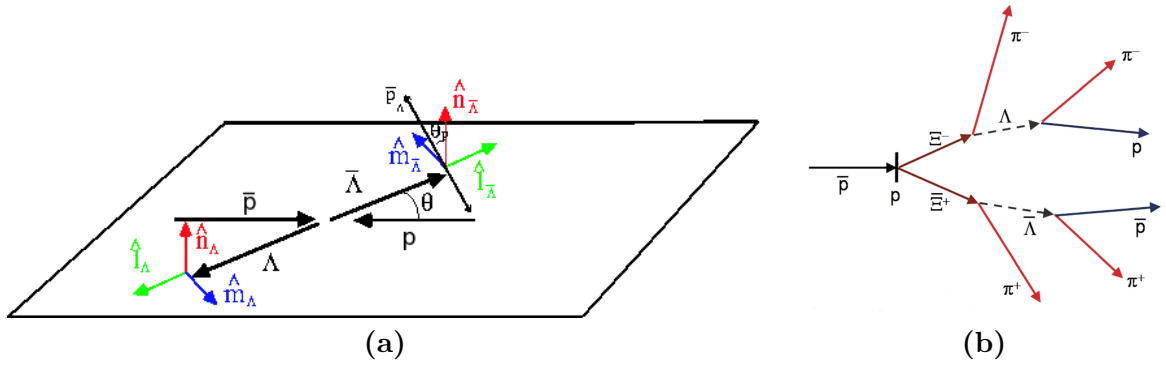

Figure 1. **(a)** The reference system of $\overline{p}p \to \overline{Y}Y$. **(b)** The $\overline{p}p \to \overline{\Xi}\Xi, \Xi \to \Lambda\pi, \Lambda \to p\pi$ decay.

2. Polarisation parameters for spin $\frac{1}{2}$ and spin $\frac{3}{2}$ hyperons

All physics information about a quantum mechanical ensemble is contained in the density matrix ρ. In an expansion in terms of hermitian matrices Q_M^L and polarisation parameters r_M^L [4], the density matrix of a particle of arbitrary spin j is given by

$$\rho = \frac{1}{2j+1} I + \sum_{L=1}^{2j} \frac{2j}{2j+1} \sum_{M=-L}^{L} Q_M^L r_M^L \tag{1}$$

where the first term denotes the unpolarised differential cross section I and the second the polarised part, containing the r_M^L parameters. L is the angular momentum and M its third component. In the case of spin $\frac{1}{2}$ particles, the Q_M^L are the Pauli matrices and the polarisation parameters correspond to the vector polarisations P_l, P_m and P_n. The indices are defined in the coordinate system shown in the left panel of figure 1. For parity conserving processes, *e.g.* $\overline{p}p \to \overline{\Lambda}\Lambda$ with unpolarised p and $\overline{p}$, symmetries of the spin density matrix imply that $P_l = P_m = 0$. This gives non-zero polarisation only perpendicular to the production plane.

The weak, parity violating decay of the hyperons means that the decay products are preferentially emitted along the direction of spin of the parent hadron. This makes the polarisation straightforward to measure. In the case of $\Lambda \to p\pi^-$, the angular distribution of the proton is related to the Λ polarisation by $I(\cos\theta_p) = \frac{1}{4\pi}(1 + \alpha_\Lambda P_n \cos\theta_p)$, where $\alpha_\Lambda = 0.64$ [5] is the asymmetry parameter. Some hyperons decay into other hyperons, *e.g.* the Ξ baryons, as illustrated in the right panel of figure 1. In the $\Xi^- \to \Lambda\pi^-, \Lambda \to p\pi^-$ process, additional asymmetry parameters β and γ of the Ξ^- hyperon are accessible *via* the angular distribution of the protons [6].

Not only the polarisation of individual hyperons $P_{y,Y}$ and antihyperons $P_{y,\overline{Y}}$ are of interest, but also the spin correlations $C_{i,j,\overline{Y}Y}$ $(i,j = x,y,z)$. These are all accessible with an unpolarised beam and an unpolarised target.

For spin $\frac{3}{2}$ hyperons, *e.g.* the Ω^-, the spin structure is more complicated. Here, we consider the polarisation parameters of individual spin $\frac{3}{2}$ hyperons only, and no correlations. The L number in equation 1 can be 1, 2 or 3 in this case. This gives three Q_M^1, five Q_M^2 and seven Q_M^3 matrices with fifteen corresponding r_M^L parameters. The corresponding spin density matrix was derived in Ref. [7]. Using symmetries imposed by strong interaction, eight polarisation parameters are identically zero.

The parameters r_0^2, r_1^2 and r_2^2 can been extracted from the angular distribution of the Λ in the $\Omega^- \to \Lambda K^-$ decay [7], assuming $\alpha_\Omega = 0$ according to previous measurements [5]. More

information about the remaining four non-zero polarisation parameters, r^1_{-1}, r^3_{-1}, r^3_{-2} and r^3_{-3}, is obtained by studying the combined angular distribution of the Λ hyperons from the Ω^- decay and the protons from the subsequent Λ decay, $I(\theta_\Lambda, \phi_\Lambda, \theta_p, \phi_p)$ [8].

3. Previous measurements

The PS185 experiment at LEAR provided high-quality data of single-strangeness hyperons (Λ and Σ) up to an antiproton beam momentum of 2 GeV/c [9]. The spin structure of the $\overline{p}p \to \overline{\Lambda}\Lambda$ reaction was explored in detail but neither quark-gluon models nor hadron models fully succeeded in explaining the behaviour of the spin observables [10]. The existing data bank on multi-strange and charmed hyperons produced in $\overline{p}p$ annihilation is scarce. A handfull of bubble chamber $\overline{p}p \to \overline{\Xi}^+\Xi^-$ events exist [11] but neither the $\overline{p}p \to \overline{\Omega}^+\Omega^-$ nor the $\overline{p}p \to \overline{\Lambda}_c^-\Lambda_c^+$ reaction have ever been observed. New experimental data could serve as a guideline for the theoretical investigation which in turn could considerably widen our understanding of the underlying processes in this energy regime.

4. Prospects for PANDA

The future PANDA experiment at FAIR opens up new possibilies in hyperon physics. The antiproton beam from the HESR storage ring, operating in a momentum range between 1.5 GeV/c and 15 GeV/c, will interact with an internal hydrogen target. The PANDA experiment will profit from the HESR high luminosity and feature a near 4π acceptance with precise tracking and vertex reconstruction, sophisticated particle identification and calorimetry [12]. Simulation studies using a simplified Monte Carlo framework [13] show excellent prospects: high signal rate, low background rate and good detection efficiency over the full phase space for all single- and multi-strange and single-charmed hyperons [7],[14]. The estimated signal rates are given in table 1. They are calculated assuming the high luminosity operating mode of HESR, corresponding to *i.e.* $2{\cdot}10^{32}\mathrm{cm}^{-2}\mathrm{s}^{-1}$, as expected in the final version of FAIR. The only well known cross section is $\overline{p}p \to \overline{\Lambda}\Lambda$ at 1.64 GeV/c; for the other strange channels the cross sections are extrapolations from data collected at other energies. For Ω and Λ_c production in $\overline{p}p$ annihilations, no data exist. The quoted values for $\sigma(\overline{p}p \to \overline{\Omega}^+\Omega^-)$ and $\sigma(\overline{p}p \to \overline{\Lambda}_c^-\Lambda_c^+)$ represent a mean value of different theoretical calculations which can differ by even an order of magnitude [15],[16].

Table 1. Approximate foreseen production rates of various hyperon channels [7],[14]. The cross sections marked with a * have a very large uncertainty. Details are given in the text.

Beam mom. (GeV/c)	Reaction	σ (μb)	Eff (%)	Decay	Rate at $2{\cdot}10^{32}\mathrm{cm}^{-2}\mathrm{s}^{-1}$
1.64	$\overline{p}p \to \overline{\Lambda}\Lambda$	64	11	$\Lambda \to p\pi^-$	580 s^{-1}
4	$\overline{p}p \to \overline{\Lambda}\Sigma^0$	$\approx$40	31	$\Sigma^0 \to \Lambda\gamma$	600 s^{-1}
4	$\overline{p}p \to \overline{\Xi}^+\Xi^-$	$\approx$2	19	$\Xi^- \to \Lambda\pi^-$	30 s^{-1}
12	$\overline{p}p \to \overline{\Omega}^+\Omega^-$	$\approx$0.002*	$\approx$30	$\Omega \to \Lambda K^-$	$\approx$80 h^{-1}
12	$\overline{p}p \to \overline{\Lambda}_c^-\Lambda_c^+$	$\approx$0.1*	$\approx$35	$\Lambda_c \to \Lambda\pi^+$	$\approx$25 d^{-1}

Spin observables of Λ, Σ, Ξ, Ω and Λ_c hyperons have also been studied. Since no data on spin variables exist for these channels, a parametrisation based on sine functions was used. In this way, the functions are equal to 0 at $\cos\theta_Y = \pm 1$ which is required by the definition of the production plane (see figure 1). More specifically, the examples shown in figure 2 are obtained with parameterisations using $P_{y,\Xi} = \sin 2\theta_\Xi$, $C_{xz,\Xi} = \sin\theta_\Xi$ and $r^2_{0,\Omega} = \sin 2\theta_\Omega/\sqrt{3}$. These reconstructed spin observables show that their measurement can be satisfactorily performed with PANDA.

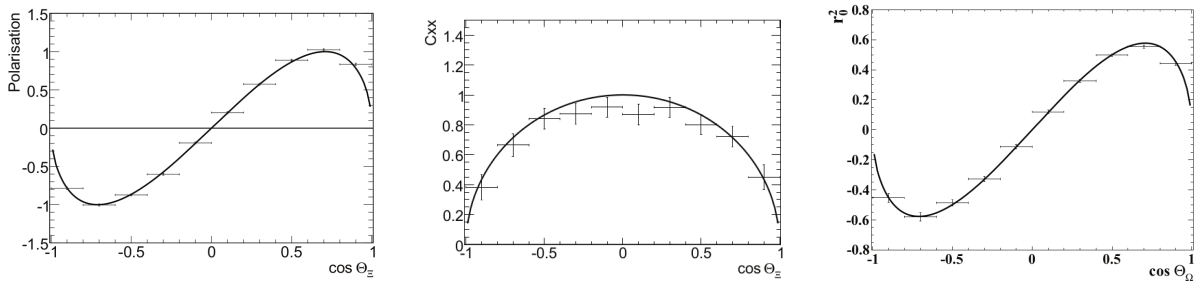

(a) **(b)** **(c)**

Figure 2. **(a)** The polarisation of the Ξ^- as a function of $\cos\theta_\Xi$. **(b)** The spin correlation in the x direction (m in Fig. 1) of the $\overline{\Xi}^+$ and the Ξ^-. **(c)** The polarisation parameter r_0^2 of the Ω as a function of $\cos\theta_\Omega$. The lines represent the input sine functions (see text) and the points and bars the reconstructed values for 10000 simulated events.

5. Summary and Outlook

The future PANDA experiment at FAIR will have a unique opportunity to give new insights into the strong interaction in the confinement domain. Spin observables in antihyperon-hyperon production provide a powerful tool for this purpose. In PANDA, the $\overline{p}p \to \overline{\Omega}^+\Omega^-$ and the $\overline{p}p \to \overline{\Lambda}_c^-\Lambda_c^+$ reaction will be studied for the first time. It will also be possible to measure the seven non-zero polarisation parameters of the Ω^- baryon that have recently been derived. The large foreseen hyperon data samples from PANDA could also open up the possibility of precise CP violation tests, hyperon Dalitz decays and other rare hyperon decays.

References

[1] Kohno M and Weise W, 1986 *Phys. Lett.* B **179** 15; Rubinstein H R and Snellman H 1985 *Phys. Lett.* B **165** 187; Furui S and Faessler A 1987 *Nucl. Phys.* A **486** 669; Burkardt M and Dillig M 1988 *Phys. Rev.* C **37** 1362; Alberg M A *et al.* 1988 *Z. Phys.* A **331** 207.
[2] Tabakin F and Eisenstein R A 1985 *Phys. Rev.* C **31** 1857; Kohno M and Weise W, 1986 *Phys. Lett.* B. **179** 15; La France P *et al.* 1988 *Phys. Lett.* B **214** 317; Timmermans R G E *et al.* 1992 *Phys. Rev.* D **45** 2288; Haidenbauer J *et al.* 1992 *Phys. Rev.* C **46** 2516.
[3] Ortega P G *et al.* 2011 *Phys. Lett.* B. **696** 352.
[4] Doncel M G *et al.* 1972 *Nucl. Phys* B **38** 477; Doncel M G *et al.* 1973 *Phys. Rev.* D **7** 815.
[5] Yao W M *et al.* [Particle Data Group] 2006 *J. Phys.* G **33** 1.
[6] Koch W 1968 *Analysis of scattering and decay* ed. Nikolic M (New York-London-Paris:Gordon and Breach).
[7] Thomé E 2012 *Multi-Strange and Charmed Antihyperon-Hyperon Physics for PANDA* Ph. D. Thesis, Uppsala University.
[8] Thomé E 2014 *A Method for Measurement of Polarisation Parameters in the* $\overline{p}p \to \overline{\Omega}^+\Omega^-$ *Reaction* (in preparation).
[9] Johansson T 2003 Antihyperon-hyperon production in antiproton-proton collisions *AIP Conf. Proc. 8th Int. Conf. on Low Energy Antiproton Physics* p 95.
[10] Klempt E *et al.* 2002 *Phys. Rep.* **368** 119.
[11] Musgrave B and Petmezas G 1965 *Nuovo Cim.* **35** 735; Baltay C *et al.* 1965 *Phys. Rev.* B **140** 1027.
[12] The PANDA collaboration, Technical Progress Report (2005).
[13] The PANDA collaboration, Physics Performance Report (2009) 43.
[14] Grape S 2009 *Studies of PWO Crystals and Simulations of the* $\overline{p}p \to \overline{\Lambda}\Lambda, \overline{\Lambda}\Sigma^0$ *Reactions for the PANDA experiment* Ph.D. Thesis, Uppsala University.
[15] Kaidalov A B and Volkovitsky P E 1994 *Z. Phys.* C **63** 51
[16] Titov A I and Kämpfer B 2008 *Phys. Rev.* C **78** 025201; Gornitschnig A T *et al.* 2009 *Eur. Phys. J.* A **42** 43; He J *et al.* 2011 *Phys. Rev.* D **84** 114010; Khodjamirian A *et al.* 2012 *Eur. Phys. J.* A **48** 31.